Using a Targeted Chemical Nuclease To Elucidate Conformational Changes in the *E. coli* 30S Ribosomal Subunit†

Gregory W. Muth,‡ Scott P. Hennelly,§ and Walter E. Hill*,§

Department of Chemistry and Division of Biological Sciences, The University of Montana, Missoula, Montana 59812

Received October 11, 1999; Revised Manuscript Received February 4, 2000

ABSTRACT: Determining the detailed tertiary structure of 16S rRNA within 30S ribosomal subunits remains a challenging problem. The particular structure of the RNA which allows tRNA to effectively interact with the associated mRNA during protein synthesis remains particularly ambiguous. This study utilizes a chemical nuclease, 1,10-*o*-phenanthroline−copper, to localize regions of 16S rRNA proximal to the decoding region under conditions in which tRNA does not readily associate with the 30S subunit (inactive conformation), and under conditions which optimize tRNA binding (active conformation). By covalently attaching 1,10-phenanthroline−copper to a DNA oligomer complementary to nucleotides in the decoding region (1396−1403), we have determined that nucleotides 923−929, 1391−1396, and 1190−1192 are within approximately 15 Å of the nucleotide base-paired to nucleotide 1403 in inactive subunits, but in active subunits only cleavages (1404−1405) immediately proximal to the 5′ end of the hybridized probe remain. These results provide evidence for dynamic movement in the 30S ribosomal subunit, reported for the first time using a targeted chemical nuclease.

Although recent crystallographic studies have provided structures at about 5 Å for both the 50S (*1*) and 30S (*2*) ribosomal subunits, and to 7.8 Å for the 70S ribosome (*3, 4*), to further understand the process of protein synthesis by the ribosome it will be necessary to know the discrete interactions between the mRNA, tRNA, and the ribosome at each instance during the process of protein synthesis. Since the ribosome is a dynamic molecule, it is essential that additional techniques to study ribosome structure be able to elucidate such structural changes. We demonstrate here the use of chemical cleavage to map dynamic interactions between the decoding region in 30S subunits and regions proximal.

The efficient binding of tRNA to 30S ribosomal subunits is often used as a standard to define translationally active subunits. The conditions for activating 30S ribosomal subunits to allow optimal tRNA binding were established early by Zamir (*5*), in which the critical concentrations of mono- and divalent cations, particularly magnesium, were identified, as well as the need to warm the subunits for a brief time. It was also demonstrated that such activation was reversible.

Details of the structural interconversion that occurs between active and inactive ribosomal subunits were initially studied using chemical modification reagents. Pioneering studies by Moazed and Noller of the active/inactive transition using chemical modification described distinct changes in the decoding region of 30S subunits upon activation of the subunits, and suggested a possible reciprocal interconversion between two structured states (*6*). Region 28 of 16S rRNA, which includes nucleotides 921−925 and 1391−1396, has been further studied in the active/inactive conformations by Wollenzien's group. In initial studies, using psoralen cross-linking, they showed that a portion of the 920 region was base-paired to the 1530 region when the 30S ribosomal subunit was in the inactive state (*7*). In more recent studies, using mutated rRNA paired with chemical probing, they established that additional structural changes in region 28 were also involved in the active/inactive transition (*8*). These studies provided evidence for an alternative arrangement of nucleotides 921−923 base-pairing with nucleotides 1532−1534.

Dramatic evidence for substantial conformational change between active and inactive subunits was published by Frank's group using the elegant technique of cryoelectron microscopy. These data provided snapshots of the 30S subunit which showed conformational changes in the head, platform, and cleft regions (*9*).

Chemical nucleases have been used previously to study ribosomal structure, especially by Noller's group (*10*−*17*). Using Fe-EDTA, Noller's group has identified regions of rRNA proximal to proteins and other regions of rRNA. In one study, they used an affinity-selection process to isolate ribosomes which had been cleaved by Fe-EDTA (*18*).

In recent years, we have used complementary DNA oligomer probes to study dynamic changes in rRNA structure (*19*). In a comprehensive DNA oligomer probing study of the decoding region and surrounds, it was demonstrated that binding of oligomers complementary to nucleotides 1397−1404 in 16S rRNA was unaffected by the activation of 30S subunits, but the binding of short DNA oligomers complementary to nucleotides in the regions of 919−928 and 1384−1417 was dramatically altered when the subunits were activated (*19*).

† Supported by a grant from the National Institutes of Health (NIGMS 35717).

* To whom correspondence should be addressed. E-mail: bi_weh@selway.umt.edu.

‡ Department of Chemistry.

§ Division of Biological Sciences.

10.1021/bi992362t CCC: $19.00
Published on Web 03/16/2000

In the present study, we have continued the use of DNA oligomers complementary to the decoding region (1396−1403), but modified with the cleavage reagent 1,10-phenanthroline covalently attached to the 5′ end of the DNA. This approach allows us to deliver the cleavage reagent to a specific region within native 30S ribosomal subunits and conduct cleavage experiments under physiological conditions. Using this approach, we have demonstrated that the cleavage patterns are altered substantially by conformational changes within ribosomal structure. Since phenanthroline−Cu(II) shows significant preference for cleaving strained, single-stranded regions of rRNA (*20*), potentially even a conformational change between an open conformation and a base-paired conformation could be discriminated. In addition, since the mechanism of cleavage by phenanthroline−Cu(II), under the conditions employed in this study, does not involve the diffusion of a hydroxyl radical, we can report the distances from the tethered site of phenanthroline−Cu(II) to the cleavage site to be no greater than 15 Å.

MATERIALS AND METHODS

5′-Thiophosphate-DNA. The complementary DNA probes were prepared in the Murdock Molecular Biology Facility, The University of Montana, using automated phosphoramidite chemistry. The solid support column 3′-dT-CPG (Glen Research, Sterling, VA) yielded a 2′-OH and a 3′-deoxy. After the addition of the final nucleotide in the sequence, an additional round of synthesis was conducted using a chemical phosphorylizing reagent (Glen Research) followed by oxidation using a sulfurizing reagent (Glen Research), yielding a 5′-PO_3S group. The sequences of each DNA oligomer are as follows: probe complementary to the decoding region nucleotides 1396−1403, GGCGGTGT; and mismatch probe, GAGAGAGAT.

5-Iodoacetamido-1,10-o-phenanthroline-5′-thiophosphate-DNA (oP-DNA). A solution of 5-iodoacetamido-1,10-phenanthroline (Molecular Probes, Eugene, OR) (200 nmol) in dimethyl sulfoxide (DMSO) was added to a 1:1 DMSO/water solution containing 20 nmol of 5′-thiophosphate-DNA, 0.1 mg of $NaBH_4$, and 1% $NaHCO_3$. The reaction was complete after 3 h at room temperature. The solvent was removed in vacuo and the residue dissolved in 50 μL of H_2O. The modified DNA was purified by chromatography (3 × 50 μL H_2O washes, Bio-Spin 6 Chromatography Column, Bio-Rad Laboratories, Hercules, CA; 1100*g*, 5 min), yielding 40−57%. Gel electrophoresis [12% acrylamide, 0.1 mg of [(*N*-acryloylamino)phenyl]mercuric chloride (APM), 10 mA, 30 min] showed a single product and the absence of starting material.

Cleavage of Ribosomal Subunits. Ribosomal subunits were isolated by a method derived from Tam (*21*) and Lodmell (*22*) from early log phase *E. coli* MRE600 bacteria and stored at −86 °C in buffer (10 mM Tris-HCl, pH 7.4, 100 mM KCl, 1.5 mM $MgCl_2$). This method of preparation ensured all subunits to be in the inactive state. Subunit homogeneity was confirmed by analytical ultracentrifugation (Model E). Ribosomal subunits were activated by heating at 37 °C for 20 min in 10 mM Tris-HCl, pH 7.4, 150 mM KCl, 15 mM $MgCl_2$ (*5*). Purified ribosomal subunits (25 pmol), both active and inactive, were added to a solution of copper sulfate (500 pmol) and oP-DNA (250 pmol) buffered in 40 mM Tris-HCl, pH 7.4, 100 mM KCl (final $MgCl_2$ concentrations were 2, 5, 10, and 15 mM) in a final volume of 10 μL. Incubation for 3 h at 0 °C ensured annealing of the oP-DNA to the complementary region of the rRNA. Addition of 3-mercaptopropionic acid (MPA) (1 mM) initiated cleavage (0 °C, 1 h). The reaction was quenched by the addition of 100 μL of precipitation buffer (70% ethanol, 8.4 mM NaOAc, pH 5, 0.8 mM EDTA). Ribosomal proteins were removed by phenol extraction, and the purified RNA was sequenced by primer extension (*23*).

RESULTS

The DNA oligomers for this study were prepared and modified at the 5′ end as outlined under Materials and Methods. To prevent reverse transcriptase (RT) from initiating transcription on the DNA probe during primer extension analysis of the rRNA, all DNA probes were synthesized with a 3′-deoxyribose. The DNA oligomers containing the 5′-phosphorothioate group were reacted with 5-iodoacetamido-1,10-phenanthroline (IoP). A mock IoP-probe control was created by reacting IoP with a 5′-phosphate probe of the same sequence to determine if the observed cleavages could be attributed to modifications to the probe other than the intended reaction. We observed no cleavages using this mock probe (data not shown).

To establish the specificity of probe binding, the ribosome−oP-DNA conjugates were incubated in the presence of RNaseH. RNaseH cleavage conducted on DNA-oP conjugates complementary to nucleotides in the decoding region (1396−1403) showed binding in a single region revealed by scission of nucleotides 1400−1401. These results indicated the probe was bound in the desired position. No additional RNaseH cleavages were observed upon sequencing the entire 16S rRNA, nor were RNaseH cleavages noted for the probe with a mismatch control sequence (data not shown). The use of untethered IoP, untethered IoP + complementary 5′-phosphate probe, and complementary 5′-phosphate probe alone provided controls for nonspecific phenanthroline cleavage, cleavage due to probe-induced RNA distortion, and possible artifacts created in primer extension analysis. No cleavages from these controls were observed in the reported regions. All cleavages attributed to IoP-DNA were attenuated completely in competition reactions where an excess of 5′-phosphate probe was annealed simultaneously with IoP-DNA probe (data not shown). The complementary probe with IoP covalently attached to the 5′ end produced dramatic cleavages at nucleotides 1404−1405 (Figure 1), further corroborating that the modified probe was bound at the desired position within the 30S ribosomal subunit. A mismatch probe with a sequence not complementary to any sequence of nucleotides in the 16S rRNA, modified to carry phenanthroline at the 5′ end (mismatch-IoP), did not show cleavage in the 1400 region (Figure 1).

Upon sequencing the entire 16S rRNA, additional cleavages attributed to the complementary probe with IoP covalently attached to the 5′ end were observed at nucleotides 1391−1396 (Figure 1), 923−929 (Figure 2), and 1190−1192 (Figure 3). To ascertain the dynamic interactions between these sites of cleavage and the decoding region, the cleavages were conducted both by titrating the amount of Mg^{2+} present and by activating the subunits prior to the introduction of DNA probes as outlined under Materials and Methods.

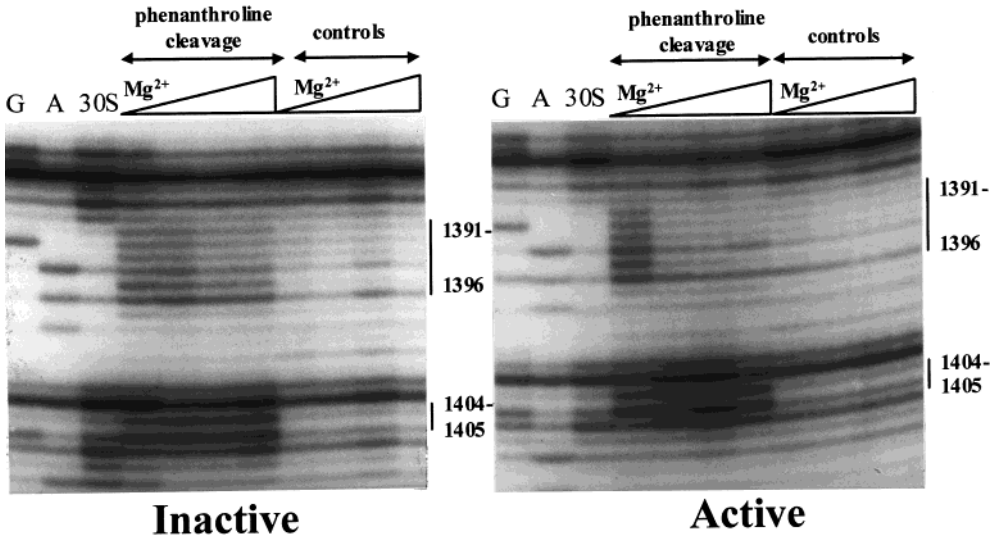

FIGURE 1: Cleavage of inactive and active 30S ribosomal subunits near the decoding region with phenanthroline covalently attached to the 5′ end of a DNA probe. G and A, sequencing lanes; 30S ribosome control, cleavage from oP-DNA probe complementary to nucleotides 1396−1403 at 2, 5, 10, and 15 mM Mg^{2+}; mismatch probe control cleavage at 2, 5, 10, and 15 mM Mg^{2+}. The subunits were activated as indicated under Materials and Methods.

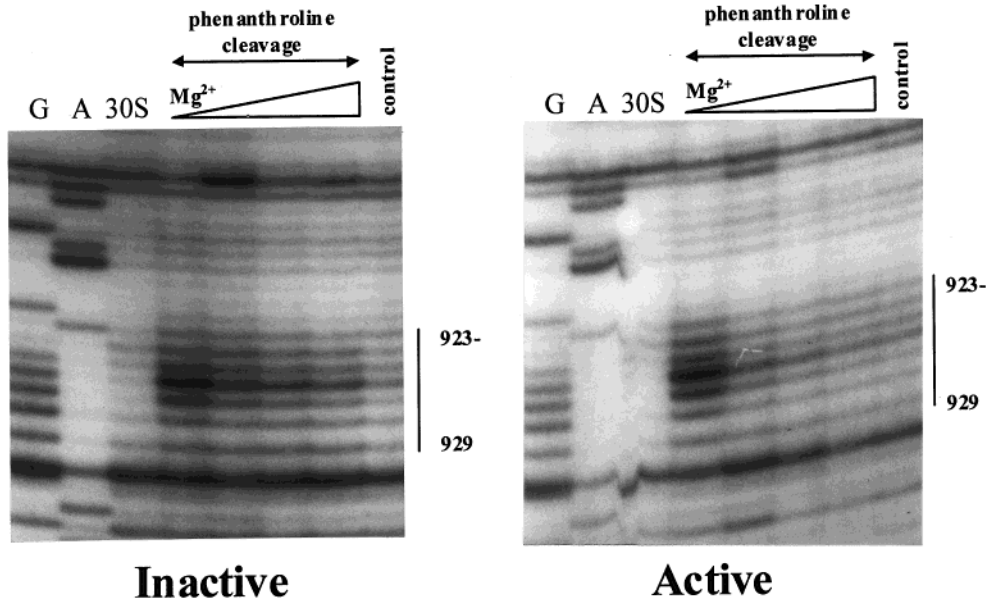

FIGURE 2: Cleavage of inactive and active 30S ribosomal subunits in the 920 region with phenanthroline covalently attached to the 5′ end of a DNA probe. G and A, sequencing lanes; 30S ribosome control, cleavage from oP-DNA probe complementary to nucleotides 1396−1403 at 2, 5, 10, and 15 mM Mg^{2+}; mismatch probe control cleavage at 2 mM Mg^{2+}. The subunits were activated as indicated under Materials and Methods.

The complementary probe−phenanthroline complex produced strong cleavages at nucleotides 1391−1396 and at nucleotides 1404−1405 of 16S rRNA when the 30S ribosomal subunits were in the inactive state (Figure 1, Inactive). The slight decrease in cleavage intensity with increasing Mg^{2+} concentration at nucleotides 1391−1396 in inactive subunits could be attributed to a slow change from inactive to active subunits, even at reduced temperatures (Figure 1, Inactive). Upon activation, the cleavage events in nucleotides 1391−1396 were absent, except at 2 mM Mg^{2+} [which is at or below the minimal magnesium concentration needed for activation (*5*)], while the cleavages at nucleotides 1404−1405 remained constant (Figure 1, Active).

The conformational transition from active to inactive was observed by conducting the cleavage reaction in buffers ranging from 2 to 15 mM $MgCl_2$. We observed that activated 30S subunits, when cleaved at 2 mM $MgCl_2$, showed the cleavage pattern observed in inactive subunits. As the Mg^{2+} concentration increased above 2 mM, cleavage decreased precipitously. This decrease can be attributed solely to a conformational change in the rRNA, since the cleavage of nucleotides 1404−1405 (proximal to the 5′ end of the IoP-oligonucleotide) remained constant at all Mg^{2+} concentrations in both the active and inactive experiments.

The cleavage events in inactive 30S subunits at nucleotides 923−929 (Figure 2, Inactive) were absent upon activation of 30S subunits, when the cleavage was conducted at Mg^{2+} concentrations >2 mM (Figure 2, Active). As with the cleavages noted at nucleotides 1391−1396 of inactive subunits (Figure 1), when the Mg^{2+} concentration was increased, a gradual decrease in cleavage intensity was noted in nucleotides 923−929 (Figure 2, Inactive). This again

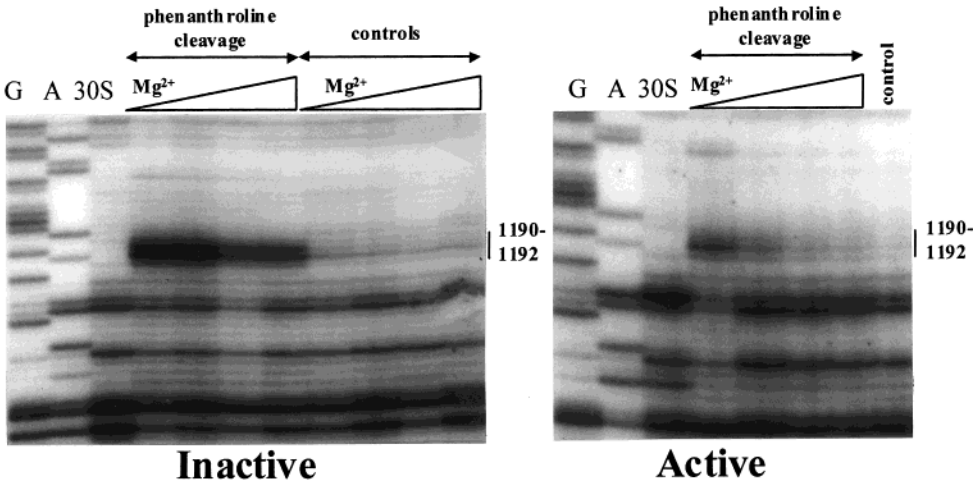

FIGURE 3: Cleavage of inactive and active 30S ribosomal subunits in the 1190 region with phenanthroline covalently attached to the 5′ end of a DNA probe. G and A, sequencing lanes; 30S ribosome control, cleavage from oP-DNA probe complementary to nucleotides 1396−1403 at 2, 5, 10, and 15 mM Mg^{2+}; mismatch probe control cleavage at 2, 5, 10, and 15 mM Mg^{2+} (Inactive). The active frame shows cleavage from oP-DNA probe complementary to nucleotides 1396−1403 at 2, 5, 10, and 15 mM Mg^{2+}; mismatch probe control cleavage at 2 mM Mg^{2+}. The subunits were activated as indicated under Materials and Methods.

suggests a slow transition from inactive to active at reduced temperature.

In helix 34, we observed robust cleavage of nucleotides 1190−1192 in inactive 30S subunits (Figure 3, Inactive). These cleavage events likewise were markedly reduced upon activation. The inactive subunits appeared to be less sensitive to reactivation at reduced temperature, showing only slight reduction in cleavage intensity with increasing Mg^{2+} concentrations. Again, when cleavage was conducted with active 30S subunits at low [Mg^{2+}] (2 mM), cleavages at nucleotides 1191−1192 were present (Figure 3, Active). These results suggested active 30S subunits do not maintain activity unless the Mg^{2+} concentration is maintained.

The cleavage events for both the active and inactive ribosomal subunits are summarized in Figure 4.

DISCUSSION

The results presented here demonstrate the effectiveness of a cleavage approach in documenting dynamic changes in ribosome structure. Since chemical cleavage takes place in solution, under conditions quite similar to those required for in vitro translation, this approach could prove to be applicable to more detailed studies which would identify exact portions of rRNA which move during the translational process. Such experiments are currently being conducted.

In this study, we have used the cleavage approach to identify some of the structural changes that occur upon activation of the 30S ribosomal subunit. These results corroborate results from other studies obtained using several techniques (*6*−*8*, *24*). Upon placing a phenanthroline−Cu(II) probe conjugate in the decoding region (nucleotides 1396−1403), cleavages in inactive 30S ribosomal subunits were found at positions 923−929 and 1391−1396 in helix 28 and at positions 1190−1192 in helix 34. When the 30S ribosomal subunits were activated, these cleavages were greatly attenuated or disappeared entirely. The results suggest that these changes in cleavage emanate from movement of portions of 16S rRNA relative to the decoding as activation occurs.

Positioning the Cleavage Reagent on the Ribosomal Subunit. The chemical cleavage reagent 1,10-*o*-phenanthroline−copper (oP) was positioned in the decoding region using an oP-DNA oligomer, complementary to nucleotides 1396−1403. The efficiency of binding a DNA oligomer complementary to nucleotides 1396−1403 has been reported at 100% with a 4:1 ratio of probe to 30S subunits both under active and under inactive conditions (*19*). RNaseH digests showed cleavages in the target region with the oP-DNA, but oP-mismatch oligomers showed no such cleavage pattern. The cleavage events (1404−1405) proximal to the 5′ end of the DNA oligomer also served as an excellent internal control for positioning the DNA oligomer on the 30S ribosomal subunit. Taken together, these experiments, plus a computer check for possible complementarity, certify that the probe is binding to the targeted region. Possible structural deformations of 16S rRNA due to probe binding were minimal, as judged from the untethered phenanthroline cleavage of 16S rRNA with and without probe present (*25*).

Phenanthroline Cleavage Distances. For directed phenanthroline cleavage of rRNA to take place, the phenanthroline first must be partially intercalated or "bookmarked" between stacked or bulged single-stranded bases, as described by Hermann and Heumann (*26*). Unlike EDTA−Fe(II), phenanthroline−Cu(II) cleavage apparently is not due to diffusible hydroxyl radicals (*27*). Rather it is proposed the cleavage is due to the abstraction of a hydrogen atom from the ribose moiety by a copper-bound oxo species giving rise to cleavage events no more than an estimated 2 Å from the copper in the Cu(II)−phenanthroline complex (*28*−*30*).

Our cleavage patterns consist of 2−6 bands, and are likely due to multiple "bookmarking" of the phenanthroline between adjacent bases (*26*). The distance from the 5′-phosphorothiolate of the DNA oligomer to the regions being cleaved would maximally be about 15 Å, with shorter distances and multiple bookmarking sites being possible due to rotation and flexibility in the acylamide tether.

We must also take into account the actual position of the 5′-phosphorothioate group relative to the rRNA to which the probe is bound. If we consider the A-form helix which is formed when the DNA probe is hybridized to the rRNA target, the 5′-phosphorothioate group (and the attached phenanthroline) may take 1 of 11 possible positions around

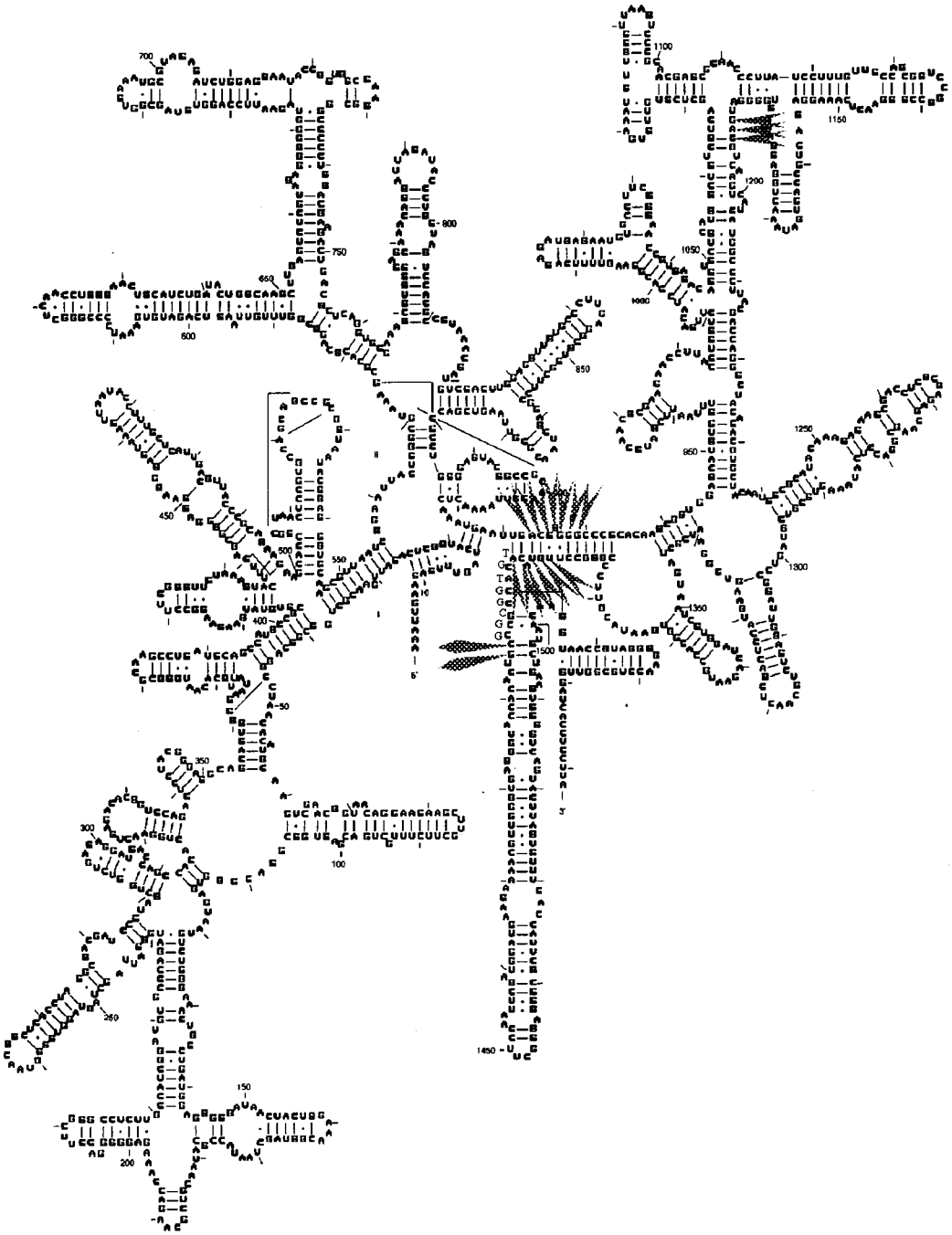

FIGURE 4: Secondary structure map of 16S rRNA from *E. coli*. The arrows map cleavage events in both active and inactive 30S ribosomal subunits from phenanthroline bound to a DNA oligomer complementary to nucleotides in the decoding region. Distance estimates place nucleotide 1403 and nucleotides 923−929, 1391−1396, and 1190−1192 within 15 Å in inactive subunits. The V-shaped symbol signifies cleavages in inactive subunits while the diamond-shaped symbol signifies cleavages independent of ribosome activation. The sequence of the complementary probe is indicated proximal to RNA bases 1396−1403.

the helical axis. It cannot be known, a priori, in which of these possible 11 positions the modified phosphorothioate group actually resides, but we do know that all of the cleavages have emanated from the phosphorothioate positioned at only 1 of the 11 positions. It is possible that regions of rRNA may be within 15 Å of the 5′ end of the probe, but these regions lie on the distal side of the rRNA/DNA hybrid, and thus would not be susceptible to cleavage. In essence, the DNA/RNA hybrid presents a barrier, behind which cleavage cannot be readily directed.

Structural Changes in the 920/1390 Regions. Using the phenanthroline−Cu(II) cleavage approach described above, we bound oP-DNA probe to the decoding site and obtained major cleavages of 16S rRNA in two different regions, in addition to the region containing nucleotides 1404−1405 adjacent to the bound phenanthroline. The 920/1390 region is part of helix 28 in 16S rRNA. This region is directly connected to the decoding site with one strand and the other to the single-stranded central hinge region which attaches the platform regions to the head. The widely accepted secondary structure map of 16S RNA shows base-pairing in helix 28 between nucleotides 1392−1396 and nucleotides 921−924.

There are several studies which suggest possible conformational changes in this region. Noller and colleagues showed that in inactive 30S subunits, nucleotides 1392 and

926 showed enhanced reactivity to chemical modifiers which was reduced upon activation (*6*). These data suggested a conformational change consisting of a single-stranded region becoming base-paired upon activation. Additional evidence for such structural changes came from psoralen cross-linking studies by Wollenzien's group, which provided evidence that the 1530 region (nucleotides 1532−1534) of 16S rRNA appeared to base-pair with nucleotides 921−923 in the inactive conformation, but not in the active conformation (*7*). Further evidence from Wollenzien's group using site-specific mutagenesis corroborates these earlier studies (*8*). Cross-linking studies from Cooperman's group have also provided some evidence for movement in this region. They have reported 24 Å cross-links generated from a modified DNA oligomer bound to nucleotides 1397−1405 to proteins S1, S7, S18, and S21 and nucleotides 1396, 1405−1408, 1492, and 1493 using active 30S subunits. A conformational change in the decoding region occurred upon inactivation of the subunits (*31*). Previous work from our laboratory has also provided evidence for movement in this region. Analysis of the binding of short, DNA oligomers to a portion of region 28 indicated that the base-pairing between the 920 and 1390 regions was altered dramatically upon activation (*19*).

The results of the present study corroborate most of these findings. We find cleavages at nucleotides 923−929 in the inactive, but not the active, conformation. This implies that in the inactive subunit, these nucleotides must be available for partial intercalation by phenanthroline−Cu(II). Since phenanthroline−Cu(II) will not intercalate into double-stranded regions of RNA, and acts by removing the C1′ hydrogen, leading to strand scission at the site where partial intercalation does occur, our results suggest that this region is quite open and is not canonically base-paired. It is possibly single-stranded, and would likely be a structure in which the bases are splayed out, available for partial intercalation by the phenanthroline. This is true for both the 920 (nt 923−929) and the 1390 region (nt 1391−1396). Although we cannot rule out base-pairing between these two regions entirely, in the inactive form, if it is present, it would have to be in a strained form which would allow the phenanthroline to partially intercalate, or it could be transient in nature. The putative base-pairing suggested by Ericson and Wollenzien (*7*) between nucleotides 1530−1532 and 921−923 in the inactive form would be subject to the same constraints.

Upon activation, the cleavages in helix 28 disappear, suggesting either that the structure becomes protected from phenanthroline−Cu(II) cleavage or that there is movement of this region relative to the position of the probe and it can no longer be reached by the tethered phenanthroline−Cu(II) complex. Although we cannot differentiate precisely between these two possibilities, we lean to the latter. If the attenuation of cleavage were due solely to the putative base-pairing between these two regions, we would still expect to see partial intercalation of the phenanthroline with resulting cleavage at G926, which is a bulged G on the secondary map. Such strained conformations are quite susceptible to cleavage. However, the intensity of this band is no greater than the control lanes, suggesting that directed cleavage does not occur. These results imply that movement between position 1403 and this region takes place upon activation, placing the region out of range of the tethered phenanthroline−Cu(II).

The above observations regarding the dynamic structure of region 28 also corroborate the more global structural changes reported by Frank's group (*9*). Using cryo-electron microscopy and a three-dimensional reconstruction at a resolution of 37 Å, with heat-activated and nonactivated subunits, they observed marked differences in the structure of these two species. Although the resolution is not sufficient to identify specific regions, their results showed substantial movement in the cleft−platform−head region, which is where the decoding region and surrounds putatively are found.

Structural Changes in Helix 34 in the 1190 Region. The cleavages found at positions 1190−1192 in helix 34 confirm that these nucleotides are within 15 Å of the 5′-end of the DNA oligomer in inactive 30S ribosomal subunits. Although these particular nucleotides have not been found near the decoding region, there has been a substantial amount of evidence accumulating that portions of helix 34 are near the decoding region. Several cross-linking studies from Brimacombe's group have shown this region to be close to positions +7 to +9 in mRNA (*32*−*35*).

Wollenzien's group has provided further support of the proximity of helix 34 to the decoding region using messenger RNA analogues, containing 4-thiouracil residues. These were shown to cross-link between position +11 in the mRNA and nucleotides A532, C1395, and A1196 in 16S rRNA (Bhangu & Wollenzien, 1992) (*36*, *37*). Selected point mutations at position 912 in region 28 of 16S RNA produced 30S subunits in which nucleotides 1392 and 1196−1197 were shown to have increased reactivity to chemical modifiers in the restrictive or inactive mutants (*38*). Hydroxyl radical probing generated from Fe(II)−EDTA tethered to position 922 in a 16S rRNA fragment in reconstituted 30S subunits localized a cleavage event in nucleotides 1192−1198 in helix 34 (*39*). All of these results provide substantial evidence that helix 34 is proximal to the decoding region.

These results, as well as those from the cleavages in helix 28, agree substantively with the model developed by Mueller and Brimacombe using cross-linking, chemical protection, and neutron scattering to develop a very comprehensive reconstruction of the 16S rRNA within the 30S subunit. This model depicts helix 28, which connects the head of the subunit to the body, as lying close behind helix 34, with the mRNA and anticodon loops of tRNA seen in near-proximity to these regions, and with C1400 of the decoding region on the right side of the neck at the base of the cleft (*40*).

It should be noted that mutation of position 1192 of 16S RNA gives rise to spectinomycin (spc)-insensitive subunits (*41*). The binding of the aminoglycoside antibiotic spectinomycin (spc) to the 30S subunit has been shown to inhibit translation possibly due to an inhibition of EF-G association (*42*).

Nucleotides 1190−1192 in helix 34 are not base-paired, even though potential Watson−Crick interaction could occur (*43*). This suggests that this region is in a conformation in which the bases are potentially available for partial intercalation. The robust cleavage which we observed suggests that this must be so. It only occurs in the inactive conformation, suggesting either base-pairing of this region or movement of this region relative to the decoding region. Judging from the work of Frank's group (*9*), movement is more likely, since their results showed substantive movements of the head

relative to the cleft between the active and inactive subunits. It would appear, as the subunit was activated, that the platform actually moves toward the head region, with some elongation and twisting of the platform taking place. Although the resolution is not such as to place the decoding region and helix 34 directly on these micrographs, such movement could definitely cause the alteration in the cleavage pattern which we observed.

CONCLUSIONS

The results of this study, combined with those of other studies, provide definitive evidence for structural changes that occur in the 30S ribosomal subunit upon activation. Not only do local changes occur in the vicinity of the decoding region, but more global changes occur including helix 34 and the spectinomycin region of 16S rRNA.

Phenanthroline−copper is a versatile tool to elucidate structural changes within the ribosome. Reactions are conducted under physiological conditions, so the ribosome can be studied in its native environment. Since there is no diffusible hydroxyl radical generated, cleavage occurs within a 15 Å sphere, so distances can be approximated. And phenanthroline−copper cleaves RNA, DNA, and peptides, both as a footprinting reagent and as a bioconjugate, allowing study of the dynamic process of protein synthesis through initiation, elongation, and termination.

ACKNOWLEDGMENT

We are indebted to Martha Rice for her technical assistance, to William Knight for his programming excellence, and to Dr. David Sigman for very helpful discussions concerning the chemistry of phenanthroline−copper cleavage.

REFERENCES

1. Ban, N., Nissen, P., Hansen, J., Capel, M., Moore, P. B., and Steitz, T. A. (1999) *Nature 400*, 841−847.
2. Clemons, W. M. J., May, J. L., Wimberly, B. T., McCutcheon, J. P., Capel, M. S., and Ramakrishnan, V. (1999) *Nature 400*, 833−840.
3. Cate, J. H., Yusupov, M. M., Yusupova, G. Z., Earnest, T. N., and Noller, H. F. (1999) *Science 285*, 2095−2104.
4. Culver, G. M., Cate, J. H., Yusupova, G. Z., Yusupov, M. M., and Noller, H. F. (1999) *Science 285*, 2133−2136.
5. Zamir, A., Miskin, R., and Elson, D. (1971) *J. Mol. Biol. 60*, 347−364.
6. Moazed, D., Van Stolk, B., Douthwaite, S., and Noller, H. F. (1986) *J. Mol. Biol. 191*, 483−493.
7. Ericson, G., and Wollenzein, P. (1989) *J. Biol. Chem. 264*, 549−545.
8. Ericson, G., Minchew, P., and Wollenzien, P. (1995) *J. Mol. Biol. 250*, 407−419.
9. Lata, K. R., Agrawal, R. K., Penczek, P., Grassucci, R., Zhu, J., and Frank, J. (1996) *J. Mol. Biol. 262*, 43−52.
10. Allen, P. N., and Noller, H. F. (1989) *J. Mol. Biol. 208*, 457−468.
11. Heilek, G. M., Marusak, R., Meares, C. F., and Noller, H. F. (1995) *Proc. Natl. Acad. Sci. U.S.A. 92*, 1113−1116.
12. Heilek, G. M., and Noller, H. F. (1996) *Science 272*, 1659−1662.
13. Huttenhofer, A., and Noller, H. F. (1992) *Proc. Natl. Acad. Sci. U.S.A. 89*, 7851−7855.
14. Newcomb, L. F., and Noller, H. F. (1999) *Biochemistry 38*, 945−951.
15. Newcomb, L. F., and Noller, H. F. (1998) *RNA '98 1*, 506 (Abstract).
16. Powers, T., and Noller, H. F. (1995) *RNA 1*, 194−209.
17. Samaha, R. R., Joseph, S., O'Brien, B., O'Brien, T. W., and Noller, H. F. (1999) *Proc. Natl. Acad. Sci. U.S.A. 96*, 366−370.
18. Noller, H. F., Green, R., Heilek, G., Hoffarth, V., Huttenhofer, A., Joseph, S., Lee, I., Lieberman, K., Mankin, A., and Merryman, C. (1995) *Biochem. Cell Biol. 73*, 997−1009.
19. Weller, J. W., and Hill, W. E. (1992) *Biochemistry 31*, 2748−2757.
20. Hermann, T., and Heumann, H. (1995) *RNA 1*, 1009−1017.
21. Tam, M. F., and Hill, W. E. (1981) *Biochemistry 20*, 6480−6484.
22. Lodmell, J. S., Tapprich, W. E., and Hill, W. E. (1993) *Biochemistry 32*, 4067−4072.
23. Moazed, M., Stern, S., and Noller, H. F. (1986) *J. Mol. Biol. 187*, 399−416.
24. Lata, K. R., Agrawal, R. K., Penczek, P., Grassucci, R., Zhu, J., and Frank, J. (1996) *J. Mol. Biol. 262*, 43−52.
25. Muth, G. W., Hennelly, S. P., and Hill, W. E. (1999) *RNA 5*, 856−864.
26. Hermann, T., and Heumann, H. (1995) *RNA 1*, 1009−1017.
27. Johnson, G. R. A., and Nazhat, N. B. (1987) *J. Am. Chem. Soc. 109*, 1990−1994.
28. Gallagher, J., Chen, C. B., Pan, C. Q., Perrin, D. M., Cho, Y.-M., and Sigman, D. S. (1996) *Bioconjugate Chem. 7*, 413−420.
29. Chen, T., and Greenberg, M. M. (1998) *J. Am. Chem. Soc. 120*, 3815−3816.
30. Meijler, M. M., Zelenko, O., and Sigman, D. S. (1997) *J. Am. Chem. Soc. 119*, 1135−1136.
31. Muralikrishna, P., and Cooperman, B. S. (1994) *Biochemistry 33*, 1392−1398.
32. Rinke-Appel, J., Junke, N., Stade, K., and Brimacombe, R. (1991) *EMBO J. 10*, 2195−2202.
33. Rinke-Appel, J., Jünke, N., Brimacombe, R., Dokudovskaya, S., Dontsova, O., and Bogdanov, A. (1993) *Nucleic Acids Res. 21*, 2853−2859.
34. Sergiev, P. V., Lavrik, I. N., Wlasoff, V. A., Dokudovskaya, S. S., Dontsova, O. A., Bogdanov, A. A., and Brimacombe, R. (1997) *RNA 3*, 464−475.
35. Dontsova, O., Dokudovskaya, S., Kopylov, A., Bogdanov, A., Rinke-Appel, J., Jünke, N., and Brimacombe, R. (1992) *EMBO J. 11*, 3105−3116.
36. Bhangu, R., Jusamiene, D., and Wollenzien, P. (1994) *Biochemistry 33*, 3063−3070.
37. Juzumiene, D., and Wollenzien, P. (1997) *Nucleic Acids Symp. Ser. 36*, 168−170.
38. Lodmell, J. S., and Dahlberg, A. E. (1997) *Science 277*, 1262−1267.
39. Samaha, R. R., Joseph, S., O'Brien, B., O'Brien, T. W., and Noller, H. F. (1999) *Proc. Natl. Acad. Sci. U.S.A. 96*, 366−370.
40. Mueller, F., and Brimacombe, R. (1997) *J. Mol. Biol. 271*, 524−544.
41. Sigmund, C. D., Ettayebi, M., Borden, A., and Morgan, E. A. (1988) *Methods Enzymol. 164*, 673−690.
42. Bilgin, N., Richter, A. A., Ehrenberg, M., Dahlberg, A. E., and Kurland, C. G. (1990) *EMBO J. 9*, 735−739.
43. Gutell, R. R. (1994) *Nucleic Acids Res. 22*, 3502−3507.

BI992362T